Alloying effect on the electronic structure of aluminium

1991 J. Phys.: Condens. Matter 3 6817

(http://iopscience.iop.org/0953-8984/3/35/011)

J. Phys.: Condens. Matter 3 (1991) 6817–6828. Printed in the UK

Alloying effect on the electronic structure of aluminium

M Morinaga†, S Nasu‡, H Adachi§, J Saito† and N Yukawa†
† Toyohashi University of Technology, Toyohashi, Aichi 441, Japan
‡ Department of Material Physics, Faculty of Engineering Science, Osaka University, Toyonaka, Osaka 560, Japan
§ Hyogo University of Teacher Education, Yashiro-cho, Kato-gun, Hyogo 673–14, Japan

Received 26 March 1991

Abstract. The influence of a number of alloying elements on the electronic structure of aluminium has been investigated by the DV-X_α cluster method. The energy level structure was modified remarkably by alloying. For transition metals, for instance, this modification was mainly due to the appearance of the virtual bound state of d electrons near the Fermi energy level. Except for a few elements, the ionicities of alloying elements change monotonically following the electronegativity. The bond order between atoms largely depends on the alloying elements, while the activation energy for the 3d impurity diffusion in aluminium can be related to the calculated bond order. An increment of the residual resistivity, due to the 3d impurities doped into aluminium, also correlates well with the virtual bound state density at the Fermi energy level. In addition, it is shown from calculations that Mn and Cr are probably the magnetic impurities in aluminium.

1. Introduction

The electronic structure of pure aluminium has been calculated by many authors (Segall 1961, Singhal and Callaway 1977, Callaway and Laurent 1981, Szmulowicz and Segall 1980, 1981, Manninen *et al* 1981, Seel 1983). The Fermi surface of aluminium is explained by a nearly-free-electron band structure (Ashcroft 1963, Ashcroft and Mermin 1976). Several experiments (e.g. optical measurements) have supported the calculated electronic structures (Szmulowicz and Segall 1981, Levinson *et al* 1983). Recently, several calculation methods for the total energy of simple metals like aluminium have been proposed (Lam and Cohen 1981, Sohoni and Kanhere 1983), and the possibility of the appearance of high-pressure phases in aluminium has been debated (Moriarty and McMahan 1982, Lam and Cohen 1983).

Steiner *et al* (1980) have investigated 3d transition-metal impurities in aluminium using x-ray photoemission spectroscopy. They have observed the Friedel–Anderson virtual bound state, which is a localized state of the d electrons existing in an aluminium s, p band (Friedel 1956, 1958a, b, Anderson 1961). Subsequent theoretical calculations have revealed the existence of such a virtual bound state, even though there are some differences among the publications as to the existing energy range and the state-density profile (Mrosan and Lehmann 1976, 1978, Nieminen and Puska 1980, Deutz *et al* 1981). Also, the virtual bound state in Al–Mn alloys has been discussed with the aid of an electron-tunnelling experiment (Terris and Ginsberg 1983). In addition, it is well known

0953-8984/91/356817 + 12 $03.50

that 3d transition-metal impurities induce a Friedel charge-oscillation in aluminium (Lautenschläger and Mrosan 1979, Lautenschläger and Plummer 1979, Mahajan and Prakash 1983).

However, there has been no systematic study of the electronic structure of Al alloyed with various transition and non-transition metals. Deutz *et al* (1981) have reported local state densities of some alloying elements in Al, but other information on the alloying behaviour still remains unknown.

Recently, Morinaga *et al* (1984a, 1985a) have investigated the electronic structure of elements in Fe, Ni and Ti alloys by using a DV-X_α cluster method. Several new alloying parameters have been obtained and used successfully in describing alloy properties. For instance, solid solubilities of FCC alloys could be elucidated well by the d-orbital energy level of alloying elements (Morinaga *et al* 1985b, c). Recently, alloying effects have been calculated in magnesium, a simple metal similar to aluminium (Morinaga *et al* 1988).

Such a theoretical calculation of alloyed Al is of great interest not only for the fundamental understanding of alloy states, but also for the practical design and development of Al alloys. In fact, we have proved the use of these calculations in developing heat-resistant Ni-based superalloys (Morinaga *et al* 1984b, Yukawa *et al* 1988).

The purpose of this paper is to calculate a series of electronic structures of Al containing both transition and non-transition metals by the discrete variational (DV) Xα cluster method. Several alloying parameters such as the s-orbital energy level, bond order, ionicity and electron density of states at the Fermi energy level, were obtained for 20 alloying elements. The alloying behaviour was estimated theoretically from these parameters. For instance, residual-resistivity changes with doped transition-metal impurities and activation energies for the impurity diffusion will be treated. A local electronic state of the magnetic impurities in aluminium will also be discussed.

2. DV-X_α cluster method and a cluster model

In this method (Slater 1974) the exchange and correlation interaction between electrons is included by means of a local exchange correlation potential, V_{xc}, which is given by

$$V_{xc} = -3\alpha[(3/8\pi)\rho(r)]^{1/3}$$

where $\rho(r)$ is the local electron density. The parameter α is fixed at 0.7 and the self-consistent charge approximation is used in the calculation. The matrix elements of the Hamiltonian and the overlap integrals are calculated by a random sampling method (Adachi *et al* 1978). The molecular orbitals are constructed by a linear combination of numerically generated atomic orbitals. For Al, the atomic orbitals used were 1s–3d, and for an alloying element M they were either 1s–*n*p ($n = 2$ for Li and Be; $n = 3$ for Na and Mg; $n = 4$ for Sc, Ti, V, Cr, Mn, Fe, Co, Ni, Cu (3d transition metals), K, Ca and Zn) or 1s–*n*d ($n = 3$ for Si and $n = 4$ for Ga and Ge). A series of calculations was carried out by a non-spin polarized method. However, a few elements (e.g. Mn) may be magnetic in Al, and hence a spin-polarized calculation was also done for several transition metals.

The energy level structure and the electron density of the states were obtained. In addition, according to a Mulliken population analysis (Mulliken 1955), the ionicity of each alloying element was estimated, and also the bond order that is a measure of the covalent bond strength between atoms, was calculated. A detailed explanation on the calculation method is given elsewhere (Adachi *et al* 1978, 1979, Morinaga *et al* 1984a, 1985a, d).

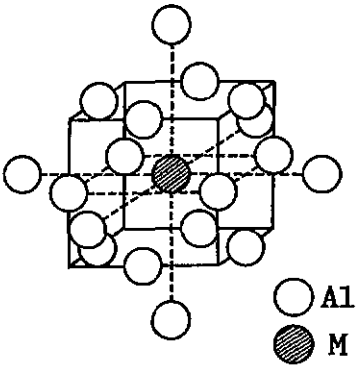

Figure 1. MAl_{18} cluster employed in the calculation.

In FCC Al, each aluminium atom is surrounded by 12 first-nearest-neighbour aluminium atoms and by six second-nearest-neighbour aluminium atoms. Therefore, the cluster employed in the present calculation was MAl_{18}, shown in figure 1. The central aluminium atom was replaced by various alloying elements, M, as described earlier. The lattice parameter used was 0.40497 nm, the same as in the bulk.

3. Results

3.1. Level structure

Some results for the level structures of Al alloyed with non-transition metals are shown in figure 2, together with the result of pure Al. In this figure, the energy, E_F, the Fermi level of pure Al, is set at zero and used as a reference. In pure Al, the levels $9a_{1g}$–$14t_{1u}$ originate mainly from the Al 3s and 3p orbitals, and form an s–p conduction band. The Fermi energy level lies on the $14t_{1u}$ level which consists of the 16.6% 3s, 80.1% 3p and 3.3% 3d components. In higher levels than E_F, there is more d component. For instance, the $2a_{2g}$ level consists of 0.0% 3s, 43.1% 3p and 56.9% 3d components. Similarly, in the $9t_{2u}$ level there are 2.4% 3s, 27.8% 3p and 69.8% 3d components.

The s component extends to a wide energy range, and its fraction of the occupancy in each level is generally small, as found for the $2a_{2g}$ and $9t_{2u}$ levels. However, in the $13a_{1g}$ level existing near 3.3 eV, there is a relatively high fraction of the s component (16.7%) which is originated from the central Al in a cluster. Although the major components are still the p (55.3%) and the d (28.0%) orbitals, the energy of this level changes systematically with alloying elements as indicated by the dotted line in figure 2. For instance, it decreases monotonously with increasing atomic number from Na to Si. For Li and Be, the $12a_{1g}$ corresponds to this level. For transition metals such a level also appears and changes systematically with the order of elements in the periodic table. Therefore, this a_{1g} level is considered to be a dominant s-component level depending on the alloying element, M, in Al. For simplicity, this level is hereafter referred to as the M-s level.

3.2. M-s level and electronegativity

As shown in figure 3, the M-s level correlates with the electronegativity of M. The electronegativity values are taken from Teatum *et al* (1968). According to Mulliken

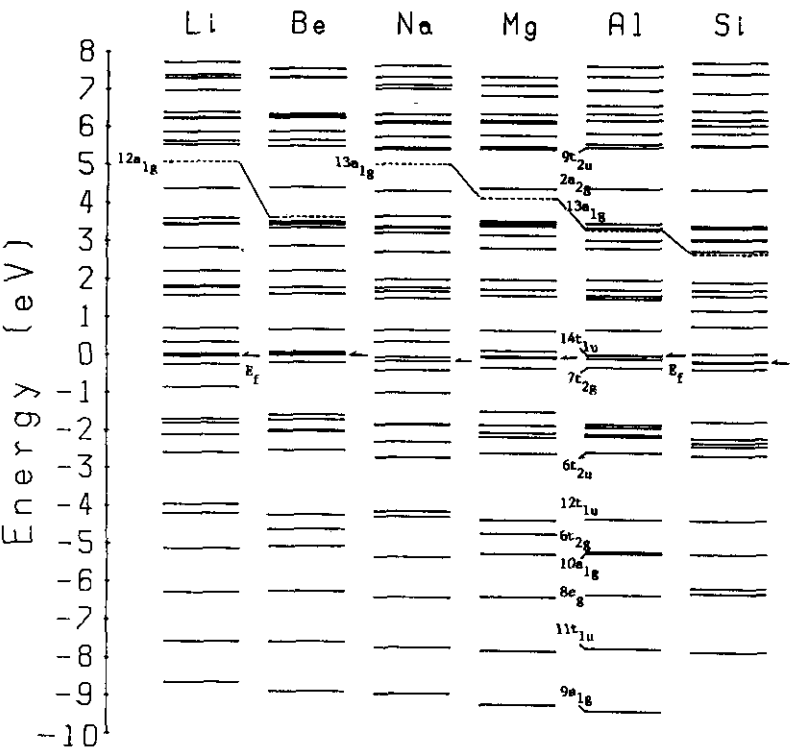

Figure 2. Energy level structures of pure and alloyed Al with non-transition metals. The Fermi level of alloyed Al is indicated by an arrow (←).

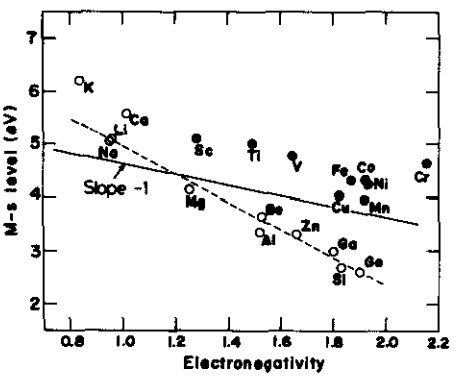

Figure 3. Correlation of M-s level with electronegativity. ●: transition metals; ○: non-transition metals.

(1955), the electronegativity of an element, ψ, is given by the arithmetic average of its first ionization energy, I, and its electron affinity, E, $\psi = (I + E)/2$. The energy eigenvalues obtained by the DV-Xα calculation represent this electronegativity, although for a cluster the covalency between neighbouring atoms necessitates some modification of this idea, as it is applied only to a free atom.

For non-transition metals (denoted by open circles in figure 3) M-s levels change linearly with the electronegativity; for transition metals (denoted by solid circles in the figure) they are located well above a dotted line of non-transition metals. This indicates

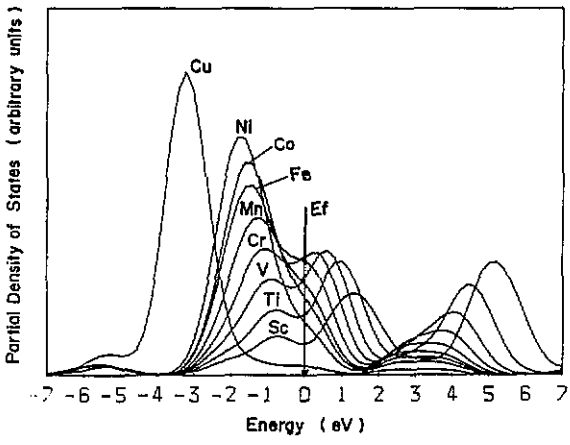

Figure 4. Partial density of states for the d electrons of transition metals in Al.

that the existence of 3d electrons affects the energy level of 4s electrons, although the reason is unknown at the moment. As a reference, a line of slope of -1 was drawn in the figure, since the M-s level (eV) may be expressed using the electronegativity, ψ (eV) as, M-s level $= -\psi + c$, where c is an arbitrary constant. This line is located between the transition metals and non-transition metals.

A similar correlation between the energy level and the electronegativity has been found in Ni alloys and Fe alloys (Morinaga *et al* 1984a, 1985a). It is very interesting to note here that this M-s level can be used in predicting mechanical properties of aluminium alloys. For example, for a variety of commercial aluminium alloys the ultimate tensile strength and the 0.2% proof strength changes linearly with the average M-s level of the alloy. A more detailed explanation will be given in a separate paper (Morinaga *et al*, to be published).

3.3. Virtual bound state

The Friedel–Anderson virtual bound state (Friedel 1956, 1958a, b, Anderson 1961) appears when transition metals are doped into Al. In figure 4, the calculated state densities of d electrons are shown for various 3d transition metals in Al. These results were obtained from overlapping Gaussian functions which have a width of 0.8 eV and their centres located at each cluster energy level (Satoko *et al* 1978).

A large single peak is observed at about -3.3 eV for Cu and at about -1.8 eV for Ni. As the atomic number decreases, the peak becomes asymmetrical (e.g. in Co and Fe), and a double-hump peak is observed (e.g. in Mn, Cr, V, Ti, Sc). At the same time, the energy for the peak shifts towards the Fermi energy level, E_F. This result is in contrast to the jellium calculation by Nieminen and Puska (1980), which shows a single peak with a Lorentzian lineshape even for Ti. Our result resembles the calculation by Deutz *et al* (1981) using a KKR–Green function method. Their lineshape deviates from a Lorentzian type, and a double-hump peak is also observed, even though the shape itself is slightly different from ours. The deviation from a Lorentzian type indicates that there is a complex interaction of transition metal d states with the Al band structure, even in a nearly-free electron metal such as Al.

Steiner *et al* (1980) observed a virtual bound state through an XPS experiment. The measured peak positions (for instance, -4.5 eV for Cu and -2.4 eV for Ni) were lower

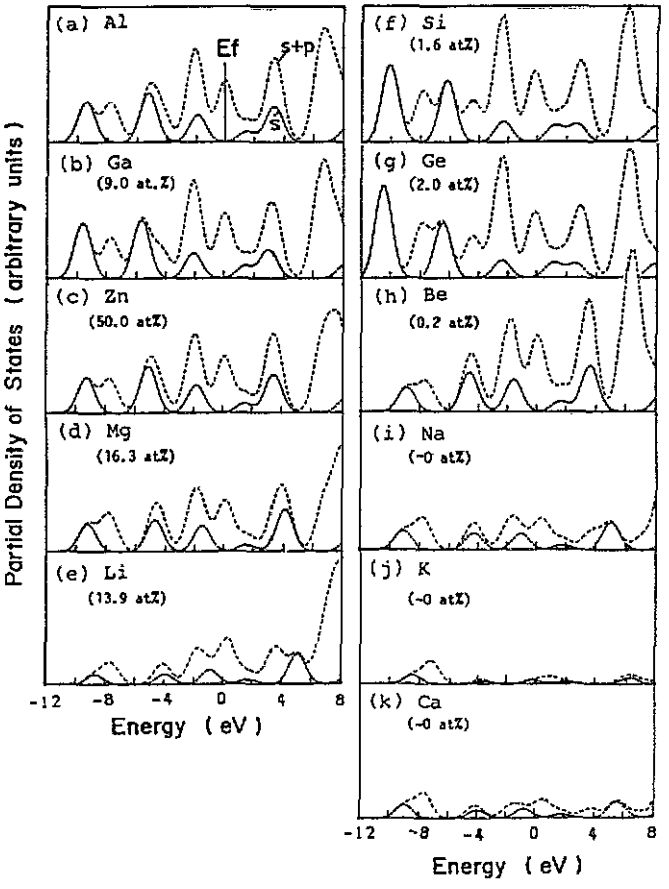

Figure 5. Partial density of states for the s and s + p electrons of non-transition metals.

than the calculated ones (−3.3 eV for Cu and −1.8 eV for Ni). Nieminen and Puska (1980) reported −3.4 eV for Cu and −1.8 eV for Ni, and Deutz *et al* (1981) reported −3.1 eV for Cu and −1.8 eV for Ni. Our results are comparable to these previous calculations, but the reason for the discrepancy between calculation and experiment is still unknown.

The existence of the virtual bound state has also been reported in magnesium (Morinaga *et al* 1988).

3.4. Partial densities of states for non-transition metals

In figure 5, the partial densities of states are compared for (*a*) Al, (*b*) Ga, (*c*) Zn, (*d*) Mg, (*e*) Li, (*f*) Si, (*g*) Ge, (*h*) Be, (*i*) Na, (*j*) K and (*k*) Ca. In the figure s and s + p denote the densities of states of the M-s and M-s + p electrons, respectively, where M is an alloying element located in the centre of a cluster. Therefore, the results of Al in figure 5(*a*) show the state densities of a central aluminium atom in the pure aluminium cluster. For a nearly-free electron metal like aluminium, the s and p energy bands are important in understanding its physical and chemical properties. Therefore, the s and p

state densities of an alloying element M are compared with those of the mother metal Al in order to examine the alloying effects on aluminium.

A solid solubility problem may be treated in terms of these state densities. When the state densities are similar between M and Al, the substitution of M for Al will not be attended by a large change in the local electronic structure. In such a case, the substitution may occur readily, resulting in a wide solubility of the element in an aluminium-rich solid solution. However, in the case when there is a large difference in the state densities, considerable modification may be made in the local electronic structure to fit the element into an aluminium site. As a result, the substitution may be suppressed, resulting in a limited solubility, or substantially no solubility, of the element in an aluminium-rich solid solution. In figure 5, a number is given in parentheses below each atomic symbol to show a maximum solid solubility (in at.%) of the element in aluminium (Massalski 1986). For instance, Ga is soluble in Al up to 9.0 at.%. In general, it may be said that high solubility elements such as Ga, Zn and Mg have state densities similar to that of aluminium, whereas low solubility elements such as Si, Ge, Na, K and Ca exhibit state densities quite different from that of aluminium. However, there are exceptions in Li and Be. Compared to Li, Be has the state density more similar to that of aluminium, but the solubility trend is the reverse. It is unknown why this discrepancy occurs. But the alloying behaviour of Li in Al seems rather peculiar, judging from the fact that the lattice constant of Al–Li alloys decreases with Li content despite the larger atomic size of Li over Al.

The solid solubility of transition elements in aluminium is very low, probably due to the appearance of the d states near E_F (see figure 4), and the resulting large incompatibility in local electronic structures. Thus, it is likely that the s, p state density is one indicator of the solid solubility of elements in aluminium. This is attributable mainly to the nearly-free electron band of aluminium.

A similar correlation has been found in a magnesium solid solution (Morinaga *et al* 1988). Instead of the present qualitative approach, the calculation of the total energy of a solid solution and the competing intermetallic compound may be the ideal approach to the solid solubility problem. However, since local lattice relaxation takes place around an impurity atom in a solid solution, the total energy should be estimated accurately including such a local strain term. In other words, the total energy should be calculated by optimizing the atomic positions around an impurity atom, but this is still very difficult at the moment.

3.5. Ionicity of elements

Charge transfer takes place between atoms in a cluster. The ionicity of each atom was evaluated from the Mulliken population analysis. As an example, the results for a series of 3d transition metals are summarized in figure 6. The ionicity of the second-nearest-neighbour aluminium, $Al^{(2)}$, is about +0.1, and shows less dependence on M. However, the ionicity of the first-nearest-neighbour aluminium, $Al^{(1)}$, correlates with that of M. Namely, the ionicity of M gradually varies following the electronegativity. For instance, Sc, the most electropositive element in the 3d series, has a positive ionicity of about +0.39, while Ni, the most electronegative element in the 3d series, has a negative ionicity of about −0.08.

3.6. Bond order

The bond order shows the overlap populations of the electrons between atoms, and that is a measure of the strength of the covalent bonding. In the present study, the bond order

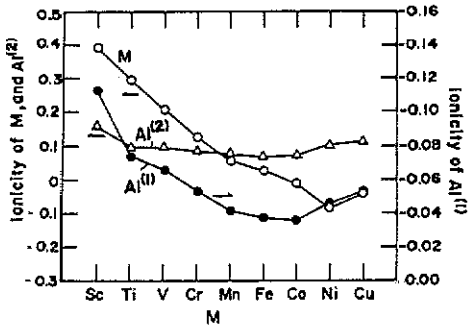

Figure 6. Ionicities of $Al^{(1)}$ atom, $Al^{(2)}$ atom and 3d transition metal M.

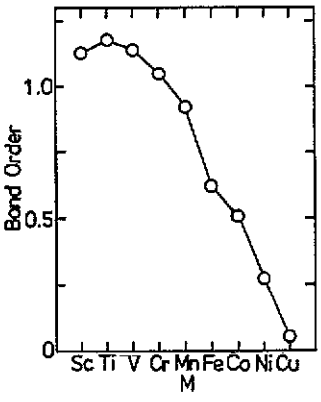

Figure 7. Bond order for 3d transition metals.

calculations were performed only for the transition metals, since for the other elements s and p electrons are the major electrons which are spread over the crystal and interact with the aluminium s and p electrons. In such a case, there may be little physical meaning in the local covalent bonding. However, for transition metals the d electrons may be localized to some extent around the atom site and interact with the aluminium s and p electrons. Therefore, the bond order was estimated as a measure of the strength of Al s, p–M-d covalent interactions. The results are shown in figure 7.

The bond order of M-Al largely depends on M. The bond order shows a broad maximum at titanium and decreases monotonously with increasing atomic number. A similar trend has also been observed in a magnesium system (Morinaga *et al* 1988).

4. Discussion

4.1. Residual resistivity

The increase of residual resistivities by the addition of 3d impurities into Al (Rizzuto 1974) has been discussed in terms of the virtual bound state. As shown in figure 8, residual resistivities show a broad peak around Cr. This is interpreted as being due to the resonance scattering of the Fermi electrons of Al by the broadened d state of the transition impurity when its energy range crosses the Fermi level of Al (Friedel 1958b). In other words, the existence of the virtual bound d state near E_F causes the scattering of the conduction electrons of Al. Therefore, high residual resistivities will be observed for those impurities which have a high density of empty d-states in the region of the Fermi energy level into which conduction electrons may be scattered (Dempsey 1963). In accordance with this inference, the calculated state density of the impurity d-electrons at the Fermi energy level, $D_d(E_F)$, correlates well with the observed resistivity as is shown in figure 8. Our result exhibits a better correlation than that by Nieminen and Puska (1980), based on the calculations of the electronic structure and the phase shift. This may be one of the examples to verify our present calculation for Al.

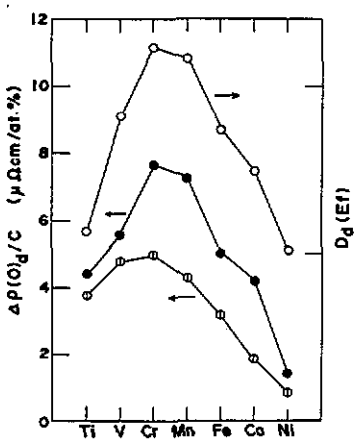

Figure 8. Increase of residual resistivity per at.% of 3d impurities ($\Delta\rho(0)_d/C$); ●: experimental value; ○: calculated state density at E_f, $D_d(E_f)$; ⊕: theoretical estimate by Nieminen and Puska (1980).

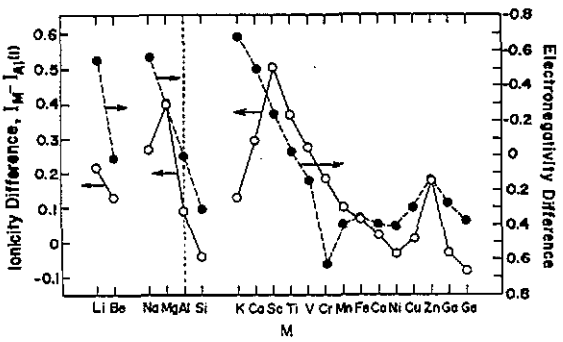

Figure 9. Ionicity difference between M and its first-nearest-neighbour aluminium atom , $Al^{(1)}$. The dashed line shows the electronegativity difference between M and $Al^{(1)}$ atoms.

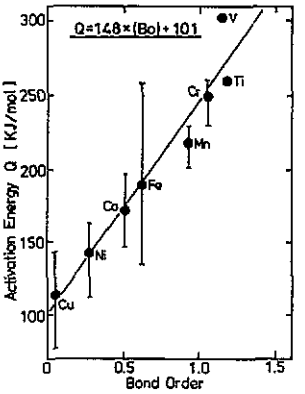

Figure 10. Correlation of the activation energies of 3d impurity diffusion in Al with the calculated bond order.

4.2. Charge transfer and bond strength

The covalent bond strength was discussed in terms of the bond order (see figure 7). In addition to this covalency, the contribution of the charge transfer to the total cohesive energy may be large in aluminium. It may increase with increasing transferred charges between atoms (Pauling 1960, Miedema 1973). In order to estimate the amount of transferred charges, the ionicity difference between M and the surrounding $Al^{(1)}$ atoms, $(I_M - I_{Al(1)})$, was calculated. The results are shown in figure 9, together with the electronegativity difference, $(\psi_M - \psi_{Al})$, (see Teatum *et al* 1968). In this figure the result of Al corresponds to the ionicity difference between a central Al atom and the surrounding $Al^{(1)}$ atoms in a pure Al cluster.

As might be expected, the ionicity difference is related to the electronegativity difference. There is a deep drop at Cr in the curve of the electronegativity difference, despite the absence of such a drop in the curve of the ionicity difference. This is probably due to the estimation methods of the electronegativity of the element. The

electronegativity for Cr reported by Watson and Bennett (1978) is intermediate between V and Mn, in coincidence with the present trend for the ionicity difference. However, for a series of K, Ca and Sc, the ionicity difference does not follow the electronegativity difference. A similar irregularity occurs for Na and Mg. This is probably due to the difference in the number of valence electrons among elements. For example, if Na and K are completely ionized, Na^{+1} and K^{+1} ions are formed and the ionicity is +1. On the other hand, for Ca and Mg the ionicity is +2, which is larger than the ionicity of Na and K. This trend appears in the calculated values of the ionicity shown in figure 9.

From these results the alloying elements expected to have a strong ionic bonding with Al are Li, Mg, Sc and Zn for each row of the periodic table. On the other hand, alloying elements which may exhibit a strong covalent bonding with Al are Sc, Ti and V as shown in figure 7. Therefore, in view of the electronic bondings with Al, the most effective elements in strengthening Al alloys may be Li, Mg, Sc, Zn, Ti and V. Some of them are in fact principal alloying elements in commercial alloys (e.g. Al–Zn–Mg). Recently, an Al–Li alloy has been studied extensively because of the high elastic modulus and low density.

4.3. Impurity diffusion in Al

It is well known that for pure metals activation energies for self-diffusion are proportional to the melting points of the metals (Askill 1970). As the melting point is probably proportional to the bond strength between atoms, the activation energy for the 3d impurity diffusion may be related to the bond order between the impurity and the mother metal. In figure 10, measured activation energies of M in Al (Mondolfo 1976, Beke *et al* 1987, Fujikawa and Hirano 1987, Minamino *et al* 1987) are plotted as a function of the bond order (see figure 7). It is interesting that there is a linear relationship between the bond order and the activation energy for the impurity diffusion in Al.

4.4. Magnetic impurities

In this study, a series of calculations was made assuming the alloying elements to be non-magnetic. This is experimentally verified for the 3d impurities in Al with the possible exceptions of Mn and Cr (Nieminen and Puska 1980). Here, the electronic structures of Mn, Cr and Fe in Al were calculated employing a spin-polarized method (Adachi *et al* 1979) and the same cluster model as in figure 1.

The local magnetic moment was calculated to be about 2.8 μ_B for Cr and 2.4 μ_B for Mn, both of which are significantly larger than 0.6 μ_B for Fe in Al, where μ_B is the Bohr magneton. This implies that Cr and Mn tend to have a localized moment and hence they are considered to be magnetic in Al, in agreement with previous discussions (Rizzuto 1974, Nieminen and Puska 1980).

The difference spin-density distribution was also obtained. This is defined as, $\Delta\rho = \rho_\uparrow(r) - \rho_\downarrow(r)$. Here, $\rho_\uparrow(r)$ and $\rho_\downarrow(r)$ are the local electron densities of up-spin and down-spin, respectively. The difference spin density distribution on the (100) atomic plane is shown in figure 11(*a*) for Mn and (*b*) for Fe. In these figures, the region where $\Delta\rho > 0$ is indicated by full curves and the region where $\Delta\rho < 0$ is indicated by broken curves. For Mn, there is a large positive peak around an Mn site, indicating that excess up-spin 3d electrons are localized and spherically distributed around an Mn site. Also, broad negative regions are extended from the central Mn site to the neighbouring aluminium sites. This indicates that down-spin electrons are distributed over the wide

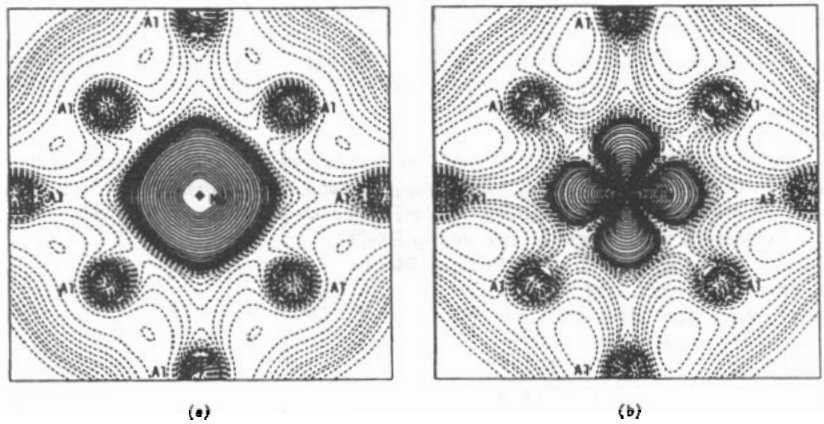

Figure 11. Difference spin-density map on the (100) atomic plane. The full curve indicates the region of excess up-spin electron density, and the broken curve indicates the region of excess down-spin electron density. The maximum values of contour lines are 0.320 electrons $(au)^{-3}$ for $MnAl_{18}$ and 0.226 electrons $(au)^{-3}$ for $FeAl_{18}$. The successive contour lines are drawn with intervals of a factor of $1/\sqrt{2}$ of each value down to the minimum values of -0.08 electrons $(au)^{-3}$ for $MnAl_{18}$ and -0.04 electrons $(au)^{-3}$ for $FeAl_{18}$.

region in a cluster. On the contrary for Fe, spin-density distributions are found to be very directional, and both up-spin and down-spin electrons are localized around an Fe site, resulting in a very low effective magnetic moment of the Fe atom.

5. Conclusions

Alloying effects on the electronic structure of aluminium have been investigated by employing a DV-Xα cluster method.

The dominant s-component level of the alloying elements appears above the Fermi energy level, E_F and changes following the electronegativity of the elements. It is confirmed that there is the virtual bound state of d electrons near the E_F for the 3d impurities in aluminium. The increase in residual resistivities due to the addition of 3d impurities is associated with the virtual bound state densities at E_F. The activation energies for the 3d impurity diffusion in aluminium are also found to be related to the calculated bond order between atoms. Furthermore, it is shown that both Mn and Cr behave like magnetic impurities in aluminium.

Acknowledgments

We would like to express our thanks to Mr K Sasaki for his assistance in the analysis of the calculated results. We also acknowledge the Computer Centre, Institute for Molecular Science, Okazaki National Research Institutes for the use of the HITAC M-680 and S-820 computers. This research was supported in part by the Grant-in-Aid for Scientific Research from the Ministry of Education, Science and Culture of Japan.

References

Adachi H, Shiokawa S, Tsukada M, Satoko C and Sugano S 1979 *J. Phys. Japan* **47** 1528
Adachi H, Tsukada M and Satoko C 1978 *J. Phys. Soc. Japan* **45** 874
Anderson P W 1961 *Phys. Rev.* **124** 41
Ashcroft N W 1963 *Phil. Mag.* **8** 2055
Ashcroft N W and Mermin N D 1976 *Solid State Physics* (New York: Holt, Rinehart and Winston) p 299
Askill J 1970 *Tracer Diffusion Data for Metals, Alloys and Simple Oxides* (New York: IFI/Plenum) p 21
Beke D L, Gödény I, Erdélyi G and Kedves F J 1987 *Materials Science Forum* vol 13/14 (Aedermannsdorf, Switzerland: Trans Tech Publications) pp 519–26
Callaway J and Laurent D G 1981 *Phys. Lett.* **84A** 499
Dempsey E 1963 *Phil. Mag.* **8** 285
Deutz J, Dederichs P H and Zeller R 1981 *J. Phys. F: Met. Phys.* **11** 1787
Friedel J 1956 *Can. J. Phys.* **34** 1190
—— 1958a *J. Phys. Radium* **19** 573
Friedel J 1958b *Suppl. Nuovo Cimento* VII 287
Fujikawa S and Hirano K 1987 *Materials Science Forum* vol 13/14 (Aedermannsdorf, Switzerland: Trans Tech Publications) pp 539–46
Lam K and Cohen M L 1981 *Phys. Rev.* B **24** 4224
—— 1983 *Phys. Rev.* B **27** 5986
Lautenschläger G and Mrosan E 1979 *Phys. Status Solidi* b **91** 109
Lautenschläger G and Plummer E W 1979 *Phys. Status Solidi* b **96** 183
Levinson H J, Greuter F and Plummer E W 1983 *Phys. Rev.* B **27** 727
Mahajan S and Prakash S 1983 *Phys. Status Solidi* b **119** 381
Manninen M, Jena P, Nieminen R M and Lee J K 1981 *Phys. Rev.* B **24** 7057
Massalski T B 1986 *Binary Alloy Phase Diagram* vols 1, 2 (Metals Park, OH: American Society of Metals) pp 20–9
Miedema A R 1973 *J. Less-Common Met.* **32** 117
Minamino Y, Yamane T, Nakagawa S, Araki H and Hirao K 1987 *Keikinzoku* **57** 72
Mondolfo L F 1976 *Aluminium Alloys: Structure and Properties* (London: Butterworths)
Moriarty J A and McMahan A K 1982 *Phys. Rev. Lett.* **48** 809
Morinaga M, Yukawa N and Adachi H 1984a *J. Phys. Soc. Japan* **53** 653
Morinaga M, Yukawa N, Adachi H and Ezaki H 1984b *Superalloys 1984* ed M Gell *et al* (Warrendale, PA: The Metallurgical Society of AIME) pp 523–32
Morinaga M, Yukawa N and Adachi H 1985a *J. Phys. F: Met. Phys.* **15** 1071
Morinaga M, Yukawa N, Ezaki H and Adachi H 1985b *Phil. Mag.* A **51** 223
—— 1985c *Phil. Mag.* A **51** 247
Morinaga M, Yukawa N and Adachi H 1985d *J. Less-Common Met.* **108** 53
Morinaga M, Yukawa N, Adachi H and Kamado S 1988 *J. Less-Common Met.* **141** 295
Mrosan E and Lehmann G 1976 *Phys. Status Solidi* b **78** 159
—— 1978 *Phys. Status Solidi* b **87** K21
Mulliken R S 1955 *J. Chem. Phys.* **23** 1833, 1841, 2339 and 2343
Nieminen R M and Puska M 1980 *J. Phys. F: Met. Phys.* **10** L123
Pauling L 1960 *Nature of the Chemical Bond* 3rd edn (Ithaca: Cornell University Press) p 92
Rizzuto C 1974 *Rep. Prog. Phys.* **37** 147
Satoko C, Tsukada M and Adachi H 1978 *J. Phys. Soc. Japan* **45** 1333
Seel M 1983 *Phys. Rev.* B **28** 778
Segall B 1961 *Phys. Rev.* **124** 1797
Singhal S P and Callaway J 1977 *Phys. Rev.* B **16** 1744
Slater J C 1974 *Quantum Theory of Molecules and Solids* vol 4 (New York: Wiley)
Sohoni G S and Kanhere D 1983 *Phys. Rev.* B **28** 3582
Steiner P, Höchst H, Steffen W and Hüfner S 1980 *Z. Phys.* B **38** 191
Szmulowicz F and Segall B 1980 *Phys. Rev.* B **21** 5628
—— 1981 *Phys. Rev.* B **24** 892
Teatum E T, Gshneidner Jr K A and Waber J T 1968 *LA-2345* (Washington, DC: US Department of Commerce)
Terris B D and Ginsberg D M 1983 *Phys. Rev.* B **27** 1619
Watson R E and Bennett L H 1978 *Phys. Rev.* B **18** 6439
Yukawa N, Morinaga M, Murata M, Ezaki H and Inoue S 1988 *Superalloys 1988* ed D N Duhl *et al* (Warrendale, PA: The Metallurgical Society of AIME) pp 225–34